The Journal of Chemical Physics

Widom insertion method in simulations with Ewald summation

Cite as: J. Chem. Phys. **156**, 134110 (2022); https://doi.org/10.1063/5.0085527
Submitted: 17 January 2022 • Accepted: 16 March 2022 • Published Online: 04 April 2022

Amin Bakhshandeh and Yan Levin

The Journal of Chemical Physics ARTICLE scitation.org/journal/jcp

Widom insertion method in simulations with Ewald summation

Cite as: J. Chem. Phys. 156, 134110 (2022); doi: 10.1063/5.0085527
Submitted: 17 January 2022 • Accepted: 16 March 2022 •
Published Online: 4 April 2022

Amin Bakhshandeh[a] and Yan Levin[b]

AFFILIATIONS

Instituto de Física, Universidade Federal do Rio Grande do Sul, Caixa Postal 15051, CEP 91501-970 Porto Alegre, RS, Brazil

[a]Electronic mail: bakhshandeh.amin@gmail.com
[b]Author to whom correspondence should be addressed: levin@if.ufrgs.br

ABSTRACT

We discuss the application of the Widom insertion method for calculation of the chemical potential of individual ions in computer simulations with Ewald summation. Two approaches are considered. In the first approach, an individual ion is inserted into a periodically replicated overall charge neutral system representing an electrolyte solution. In the second approach, an inserted ion is also periodically replicated, leading to the violation of the overall charge neutrality. This requires the introduction of an additional neutralizing background. We find that the second approach leads to a much better agreement with the results of grand canonical Monte Carlo simulation for the total chemical potential of a neutral ionic cluster.

I. INTRODUCTION

Ion chemical potential is an important thermodynamic quantity that is relevant for phase equilibrium and reaction chemistry. However, measuring the chemical potential, or equivalently, the solvation free energy of individual ions, is very difficult experimentally, requiring some specific assumptions.[1] On the other hand, the chemical potential of ions can be calculated approximately using theoretical methods, such as Mean Spherical Approximation (MSA) or Hypernetted Chain (HNC) equation.[2–4] Such approaches, however, are not exact and rely on specific closure relations of the Ornstein–Zernike equation. Therefore, it is desirable to have an "exact" method to obtain chemical potential using Monte Carlo (MC) simulations. For systems with short range interactions, there are two usual approaches: (1) grand canonical MC simulation (GCMC) and (2) the Widom insertion method.

The simulations of Coulomb systems are significantly more complicated than those of systems with short range forces. The long-range nature of the Coulomb potential precludes the use of simple periodic boundary conditions, requiring a periodic replication of the whole system. Each ion then interacts with all the other ions inside the simulation cell and also with all the periodic replicas of all these ions. To efficiently account for the periodicity of the replicated systems, the usual approach is to use Ewald summation methods.[5–16] In the thermodynamic limit, the system must be charge neutral, and the GCMC must, therefore, be implemented in such a way as to respect this requirement. The simple way to do this is to insert charge neutral clusters into the simulation box. Such an approach, however, precludes us from determining individual chemical potential of ions, allowing only the calculation of the total chemical potential of a neutral cluster. For example, in the case of α:1 electrolyte, where α refers to the cation valence, we can only determine the combination $\mu_t = \mu_+ + \alpha\mu_-$, where μ_+ and μ_- are the cation and anion chemical potentials, respectively. Therefore, such implementation of GCMC does not provide us with access to individual chemical potentials μ_+ and μ_-, but only to μ_t. We should note, however, that there is a different implementation of GCMC in which individual ions, together with their respective neutralizing background, are inserted into the simulation box.[17] The difficulty in such an approach is that the chemical potential of cations and anions must be carefully adjusted, so that neutrality of the simulation box is only due to ions and not because of an artificial background.

An alternative approach that allows us to obtain individual chemical potentials of ions is the Widom insertion method.[18] Widom showed that the chemical potential of a particle is related to the acceptance probability of inserting particle $N+1$ into the system that already contains N particles,[18–27]

$$\mu_{ex} = -k_B T \ln\left\langle \frac{1}{V}\int ds_{N+1}\, \exp(-\beta\Delta U)\right\rangle_N, \tag{1}$$

where $\Delta U \equiv U(s^{N+1}) - U(s^N)$ is the energy difference for systems with N and $N+1$ particles. The integral is easily calculate inside a canonical MC simulation by sampling the insertion probability $\exp(-\beta\Delta U)$ after the simulation with N particles has fully equilibrated.[28–32]

Widom's method has been widely used for evaluating the excess chemical potential for different systems, such as supercritical fluid-solid equilibria,[33,34] mixture of Argon and 1-magne-4-polybutadiene,[35] and binary phases.[36] The Widom insertion method was also used to calculate ionic solvation free energy in atomistic simulations.[29,37–39]

To use Eq. (1) requires calculation of ΔU, which is the change in energy of the system due to addition of a test ion. Within the Ewald summation formalism, there is, however, an ambiguity in the definition of ΔU. One way is to interpret ΔU as the energy due to the interaction of an extra ion with all the other ions inside the simulation cell, as well as with all the replicas of these ions. There is no problem with violation of charge neutrality in this case since only one extra ion is added to a charge neutral system, and this ion is not replicated. An alternative is to treat the added ion on the same footing as the other ions inside the system. In this case, both the new ion and its periodic replicas must be used to calculate ΔU. This will lead to the interaction of ion with its own replicas, resulting in a non-neutral macroscopic system with diverging electrostatic energy. To overcome this difficulty, we can add a uniform neutralizing background that is introduced simultaneously with the inserted ion. The background charge will be replicated together with the ion, preserving the overall charge neutrality. This will result in an overall charge neutral system with extensive energy. *A priori* it is not clear which one of this procedures will lead to a better approximation to the exact value of the ionic chemical potential. We should note, however, that within minimum image approximation inclusion of neutralizing background has been found to lead to much faster convergence to the thermodynamic limit.[30] In this paper, we will test both Ewald summation approaches by calculating the chemical potential of cations and anions separately and then compare the resulting value of μ_t obtained using each approach with the value of μ_t calculated using GCMC. The GCMC will provide us with a benchmark to measure the accuracy of the two Widom insertion methods for periodically replicated systems.

The rest of this paper is organized as follows: In Sec. II, we briefly review the grand canonical simulation method for α:1 electrolyte. In Sec. III, we will derive the expressions for ΔU used in the two Widom insertion methods. In Sec. IV, we will present the results of the simulations obtained using the two ΔU and compare the results with the μ_t calculated using the GCMC simulations. Finally, in Sec. V, we will discuss the conclusions of this work.

II. GRAND CANONICAL MONTE CARLO SIMULATION

To calculate μ_t, we can perform GCMC simulations for α:1 electrolyte. To this end, we use a cubic simulation cell with side length $L = 100$ Å. To account for the long range Coulomb interaction, we use the Ewald summation method for neutral systems[40,41] with the number of k-vectors around 600. The system is found to reach equilibrium after 2×10^6 MC steps. 20 000 samples are then used for the statistical analysis. In each MC move, there are three possibilities: Simple movement of ions or addition or removal of one cation and α anions, so as to preserve the overall charge neutrality of the system. The transition probability for addition of ions (from state i to j),[32,42–44]

$$\frac{\rho_j}{\rho_i} = \frac{V^{\alpha+1} e^{-\beta U_j + \beta U_i + \beta\mu_t}}{(N_+ + 1)(N_- + \alpha)(N_- + \alpha - 1)\cdots(N_- + 1)\Lambda_+^3\Lambda_-^{3\alpha}}, \quad (2)$$

where V is the volume of the simulation cell, $N_\pm$ is the number of cations and anions, U_i is the electrostatic energy of the state i, $\mu_t = \mu_+ + \alpha\mu_-$ is the total chemical potential of a minimum neutral cluster, and $\Lambda_\pm$ are the thermal de Broglie wavelengths of cations and anions. The removal probability is

$$\frac{\rho_j}{\rho_i} = \frac{e^{-\beta U_j + \beta U_i - \beta\mu_t} N_+ N_- (N_- - 1)\cdots(N_- - \alpha + 1)\Lambda_+^3\Lambda_-^{3\alpha}}{V^{\alpha+1}}. \quad (3)$$

We start with an empty simulation cell and specify μ_t of the reservoir. The simulation is then run until the equilibrium is established and the average number of cations, $\langle N_+ \rangle$, inside the simulation cell is calculated. From this, we calculate the average concentration of electrolyte $\langle c \rangle$ corresponding to a fixed value of fugacity $\exp(\beta\mu_t)/\Lambda_+^3\Lambda_-^{3\alpha}$. The excess part of the total chemical potential can then be calculated as $\mu_t^{ex} = \mu_t - \ln[\langle c \rangle^{\alpha+1}\Lambda_+^3\Lambda_-^{3\alpha}] - \alpha \ln \alpha$.

III. WIDOM INSERTION METHOD

The difficulty with applying the Widom insertion method to systems with Coulomb interactions is due to the necessity of periodic replication of the simulation box. The electrostatic potential inside the simulation cell satisfies the Poisson equation

$$\nabla^2\phi(\boldsymbol{r}) = -\frac{4\pi q_i}{\varepsilon_w}\sum_{j=1}^{N}\sum_{n_x,n_y,n_z=-\infty}^{\infty}\delta(\boldsymbol{r} - \boldsymbol{r}^j + n_x L\hat{\boldsymbol{x}} + n_y L\hat{\boldsymbol{y}} + n_z L\hat{\boldsymbol{z}}), \quad (4)$$

where ε_w is the dielectric constant of water and n's are integers corresponding to periodic replicas. Using the usual procedure, the equation can be integrated by separating the Coulomb potential into long and short range contributions. The long range contribution can be efficiently summed in the Fourier space, while the short range in the real space. The electrostatic potential can then be written as

$$\phi(\boldsymbol{r}) = \sum_{\boldsymbol{k}=\boldsymbol{0}}^{\infty}\sum_{j=1}^{N}\frac{4\pi q^j}{\varepsilon_w V|\boldsymbol{k}|^2}\exp\left[-\frac{|\boldsymbol{k}|^2}{4\kappa_e^2} + i\boldsymbol{k}\cdot(\boldsymbol{r} - \boldsymbol{r}^j)\right] + \sum_{j=1}^{N}\sum_{\boldsymbol{n}} q^j\frac{\operatorname{erfc}(\kappa_e|\boldsymbol{r} - \boldsymbol{r}^j - L\boldsymbol{n}|)}{\varepsilon_w|\boldsymbol{r} - \boldsymbol{r}^j|}, \quad (5)$$

where $\boldsymbol{n} = (n_1, n_2, n_3)$ are the integer lattice vectors and $\boldsymbol{k} = (\frac{2\pi}{L}n_1, \frac{2\pi}{L}n_2, \frac{2\pi}{L}n_3)$ are the reciprocal lattice vectors. The damping parameter κ_e is chosen so that we can replace the sum over $\boldsymbol{n}$ by a simple periodic boundary condition for the short range part of the electrostatic potential in the real space. This is possible as long as $\kappa_e > 5/L$. A special care must be taken in evaluating the $\boldsymbol{k} = \boldsymbol{0}$ term.[45] Expanding around $|\boldsymbol{k}| = 0$ this term can be written as

$$\lim_{\boldsymbol{k}\to 0}\sum_{j=1}^{N} q^j \frac{1}{|\boldsymbol{k}|^2} - \sum_{j=1}^{N} q^j \frac{1}{4\kappa_e^2} + \lim_{\boldsymbol{k}\to 0}\sum_{j=1}^{N} q^j \frac{i\boldsymbol{k}\cdot(\boldsymbol{r}-\boldsymbol{r}^j)}{|\boldsymbol{k}|^2} - \lim_{\boldsymbol{k}\to 0}\sum_{j=1}^{N} q^j \frac{[\boldsymbol{k}\cdot(\boldsymbol{r}-\boldsymbol{r}^j)]^2}{2|\boldsymbol{k}|^2}. \quad (6)$$

The first term is divergent; however, it is multiplied by $\sum_i q^i$, which, for a charge neutral system, is zero. Similarly, it is possible to show that the third term is also zero by symmetry.[45] The only non-trivial term is the last one that evaluates to a finite value, resulting in electrostatic potential at position $\boldsymbol{r}$ inside the simulation cell given by

$$\phi(\boldsymbol{r}) = \sum_{\boldsymbol{k}\neq 0}^{\infty}\sum_{j=1}^{N} \frac{4\pi q^j}{\varepsilon_w V|\boldsymbol{k}|^2} \exp\left[-\frac{|\boldsymbol{k}|^2}{4\kappa_e^2} + i\boldsymbol{k}\cdot(\boldsymbol{r}-\boldsymbol{r}^j)\right] + \sum_{j=1}^{N} q^j \sum_{\boldsymbol{n}} \frac{\operatorname{erfc}(\kappa_e|\boldsymbol{r}-\boldsymbol{r}^j-L\boldsymbol{n}|)}{\varepsilon_w|\boldsymbol{r}-\boldsymbol{r}^j|} - \sum_{j=1}^{N} \frac{2\pi q^j}{3\varepsilon_w V}(\boldsymbol{r}-\boldsymbol{r}^j)^2. \quad (7)$$

We can recognize the last term of this expression as the sum over electrostatic potentials produced by infinite uniformly charged spheres—each with charge density q_i/V—centered on positions of ions. This provides us with an interesting interpretation of Ewald summation. Effectively it replaces each ion, and its respective replicas, by infinite uniformly charged spheres centered on positions of physical ions. The discreteness effects are then encoded in the first two terms of Eq. (7), which correspond to ions inside a neutralizing background. Note that this interpretation applies also to charge non-neutral systems.[45]

For the charge neutral system, we can rewrite expression (7) as

$$\phi(\boldsymbol{r}) = \sum_{\boldsymbol{k}\neq 0}^{\infty}\sum_{j=1}^{N} \frac{4\pi q^j}{\varepsilon_w V|\boldsymbol{k}|^2} \exp\left[-\frac{|\boldsymbol{k}|^2}{4\kappa_e^2} + i\boldsymbol{k}\cdot(\boldsymbol{r}-\boldsymbol{r}^j)\right] + \frac{4\pi}{3\varepsilon_w V}\mathbf{r}\cdot\mathbf{M} - \sum_{j=1}^{N} \frac{2\pi q^j \boldsymbol{r}^j\cdot\boldsymbol{r}^j}{3\varepsilon_w V} + \sum_{j=1}^{N} q^j \sum_{\boldsymbol{n}} \frac{\operatorname{erfc}(\kappa_e|\boldsymbol{r}-\boldsymbol{r}^j-L\boldsymbol{n}|)}{\varepsilon_w|\boldsymbol{r}-\boldsymbol{r}^j|}, \quad (8)$$

where $\boldsymbol{M} = \sum_{j=1}^{N} q^j \boldsymbol{r}^j$ is the electric moment of the simulation cell with N ions and the sum over the short range interaction is performed using the simple periodic boundary condition. We recognize the $\mathbf{r}\cdot\mathbf{M}$ term as the shape dependent surface potential produced by a macroscopic ferroelectric.[46,47] The surface term is particularly important for systems with broken symmetry, such as slab geometry and ion channels.[45,48–51] For spherically symmetric bulk systems, this term, however, leads to an unrealistic net dipole moment of a macroscopic system, which is clearly absent in the disordered state of an electrolyte solution. We can remove this term by using the tin-foil boundary condition in which our macroscopic system is enclosed by a perfect conductor.[47,52] Indeed, as we will show below (see Fig. 1), the expression without the surface term results in a better agreement with the mean spherical approximation, which is exact at infinite dilution. The electrostatic energy of a charge neutral system with N ions is then

$$U_N = \frac{1}{2}\sum_{j=1}^{N} q^j \left[\phi(\boldsymbol{r}^j) - \lim_{\boldsymbol{r}\to\boldsymbol{r}^j}\frac{q^j}{|\boldsymbol{r}-\boldsymbol{r}^j|}\right]. \quad (9)$$

Using Eq. (8), this can be written as

$$U_N = \sum_{\boldsymbol{k}\neq\boldsymbol{0}}^{\infty} \frac{2\pi}{\varepsilon_w V|\boldsymbol{k}|^2} \exp\left[-\frac{|\boldsymbol{k}|^2}{4\kappa_e^2}\right][A(\boldsymbol{k})^2 + B(\boldsymbol{k})^2] + \frac{1}{2}\sum_{i\neq j}^{N} q^i q^j \frac{\operatorname{erfc}(\kappa_e|\boldsymbol{r}^i-\boldsymbol{r}^j|)}{\varepsilon_w|\boldsymbol{r}^i-\boldsymbol{r}^j|} + \frac{2\pi}{3\varepsilon_w V}|\mathbf{M}|^2 - \frac{\kappa_e}{\sqrt{\pi}}\sum_{i=1}^{N}(q^i)^2, \quad (10)$$

where

$$A(\boldsymbol{k}) = \sum_{i=1}^{N} q^i \cos(\boldsymbol{k}\cdot\boldsymbol{r}^i), \qquad B(\boldsymbol{k}) = -\sum_{i=1}^{N} q^i \sin(\boldsymbol{k}\cdot\boldsymbol{r}^i). \quad (11)$$

This is the electrostatic energy for the vacuum boundary condition, in which the surface $\mathbf{M}$ appears explicitly. On the other hand, the tin-foil boundary condition entails removal of the $|\mathbf{M}|^2$ term from Eq. (10).[47,52] We now compare μ_t^{ex} calculated using the GCMC with vacuum and the tin-foil boundary conditions for symmetric 1:1 electrolyte, with the theoretical result obtained using the Mean Spherical Approximation (MSA) with the Carnahan–Starling (CS) expression for the excluded volume interaction. The MSA + CS expression, $\mu_t^{ex} = \mu_{MSA} + \mu_{CS}$, is exact for dilute electrolyte[2,19,29,53–59] with

$$\mu_{MSA} = \frac{\lambda_B\left(\sqrt{1+2\kappa d}-\kappa d-1\right)}{d^2\kappa}, \quad (12)$$

$$\mu_{CS} = \frac{8\eta-9\eta^2+3\eta^3}{(1-\eta)^3}, \quad (13)$$

where $\eta = \frac{\pi d^3}{3} c_t$, d is the ionic diameter, $c_t = c_+ + c_-$ is the total concentration of ions, and $\kappa = \sqrt{8\pi\lambda_B c_t}$ is the inverse Debye length. In simulations, we use a cubic cell of length 100 Å.

As expected, Fig. 1 shows that Eq. (10) with tin-foil boundary condition results in a better agreement with the theoretical curve at low concentrations of electrolyte. For larger simulation cells, the difference between vacuum and tin-foil boundary condition becomes less important.

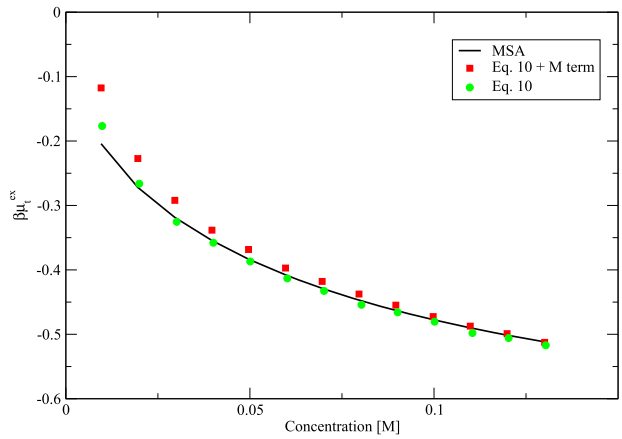

FIG. 1. Total excess chemical potential of symmetric 1:1 electrolyte calculated using GCMC simulations with electrostatic energy given by Eq. (10) with M term (vacuum boundary condition) and without M term (tin-foil boundary condition), compared with the theoretical MSA + CS result.

A. Method I

As discussed previously, we have two options for implementing the Widom insertion in a system with Ewald summation. In the first approach, we simply insert a new ion of charge Q at position $\boldsymbol{r}^i$. The change in the electrostatic energy due to the interaction of this ion with all the other ions inside the system and with their replicas is then

$$\Delta U = Q\phi(\boldsymbol{r}^i), \tag{14}$$

where $\phi(\boldsymbol{r}^i)$ is the electrostatic potential at position of insertion given by Eq. (8) without the $\mathbf{M}$ term for tin-foil boundary condition.

B. Method II

An alternative approach is to treat the inserted ion on the same footing as all the other ions inside the simulation cell—replicating it, along with all the other ions. In this case, the inserted ion will also interact with its own replicas, leading to a diverging electrostatic energy. The divergence appears in the first term of the expression (6), which is no longer zero, since there is a net charge inside the simulation cell. To overcome this difficulty, we introduce, together with the test ion of charge Q, a uniform neutralizing background of opposite charge density $\rho_b(\boldsymbol{r}) = -Q/V$, which will also be replicated together with the ions. Any periodic density function over a cubic lattice can be written as

$$\rho(\boldsymbol{r}) = \frac{1}{V}\sum_{\boldsymbol{k}}\tilde{\rho}(\boldsymbol{k})e^{i\boldsymbol{k}\cdot\boldsymbol{r}}, \tag{15}$$

with a similar expression for the electrostatic potential. The Fourier transforms of the electrostatic potential and of the charge density are

$$\begin{aligned}\tilde{\phi}(\boldsymbol{k}) &= \int_V \phi(\boldsymbol{r})e^{-i\boldsymbol{k}.\boldsymbol{r}}d^3r,\\ \tilde{\rho}(\boldsymbol{k}) &= \int_V \rho(\boldsymbol{r})e^{-i\boldsymbol{k}.\boldsymbol{r}}d^3r,\end{aligned} \tag{16}$$

where V is the volume of the simulation cell. In particular, for a uniform background charge density, we obtain $\tilde{\rho}_b(\boldsymbol{k}) = -Q\delta_{\boldsymbol{k},\boldsymbol{0}}$, where δ is the Kronecker delta. The electrostatic potential produced by the background satisfies the Poisson equation

$$\nabla^2\phi(\boldsymbol{r}) = -\frac{4\pi\rho(\boldsymbol{r})}{\varepsilon_w}. \tag{17}$$

Substituting the Fourier representation of electrostatic potential and of charge density into Eq. (17), we obtain

$$\tilde{\phi}(k) = \frac{4\pi}{\varepsilon_w}\frac{\tilde{\rho}(\boldsymbol{k})}{k^2}. \tag{18}$$

Finally, using the expression for the Fourier transform of the uniform background charge, we obtain the contribution that it produces to the total electrostatic potential,

$$\phi_b(\boldsymbol{r}) = -\frac{4\pi Q}{V\varepsilon_w}\sum_{\boldsymbol{k}}e^{i\boldsymbol{k}.(\boldsymbol{r}-\boldsymbol{r}^i)}\frac{\delta_{\boldsymbol{k},0}}{k^2}, \tag{19}$$

where we have centered the background on the position of the inserted ion. Adding this background potential to the potential produced by all $N+1$ replicated ions, we see that the divergence in the $\boldsymbol{k} = \boldsymbol{0}$ term in expression (6) cancels exactly. There is, however, now an additional term coming from the $\boldsymbol{k} \to \boldsymbol{0}$ limit of Eq. (19). This term is proportional to $(\boldsymbol{r} - \boldsymbol{r}^i)^2$ and will cancel the same term in Eq. (7) for the $N+1$ particle system, resulting in the total electrostatic potential of a system with a neutralizing background,

$$\begin{aligned}\varphi(\boldsymbol{r}) = &\sum_{\boldsymbol{k}\neq 0}^{\infty}\sum_{j=1}^{N+1}\frac{4\pi q^j}{\varepsilon_w V|\boldsymbol{k}|^2}\exp\left[-\frac{|\boldsymbol{k}|^2}{4\kappa_e^2} + i\boldsymbol{k}\cdot(\boldsymbol{r}-\boldsymbol{r}^j)\right]\\ &-\sum_{j=1}^{N}\frac{2\pi q^j}{3\varepsilon_w V}(\boldsymbol{r}-\boldsymbol{r}^j)^2 - \frac{Q}{\varepsilon_w V\kappa_e^2}\\ &+\sum_{j=1}^{N+1}\sum_{\boldsymbol{n}}q^j\frac{\operatorname{erfc}(\kappa_e|\boldsymbol{r}-\boldsymbol{r}^j-L\boldsymbol{n}|)}{\varepsilon_w|\boldsymbol{r}-\boldsymbol{r}^j|},\end{aligned} \tag{20}$$

where we have defined the $j = N+1$ as our test ion with the charge $q_{N+1} = Q$. Note that the second sum in Eq. (20) runs only over the original ions present in the system.

Suppose we insert a test ions at position $\boldsymbol{r}^i$, together with the associated neutralizing background, into an initially empty simulation cell, $N = 0$. The electrostatic energy of this system will be

$$U_0 = \frac{Q}{2}\lim_{\boldsymbol{r}\to\boldsymbol{r}^i}\left(\varphi(\boldsymbol{r}) - \frac{Q}{|\boldsymbol{r}-\boldsymbol{r}^i|}\right). \tag{21}$$

Performing the limit, we obtain

$$\beta U_0 = -1.418\,648\,739\frac{\alpha^2\lambda_B}{L}, \tag{22}$$

where α is the valence of ion of charge $Q = \alpha q$, where q is the proton charge, and $\lambda_B = q^2/\varepsilon_w k_B T$ is the Bjerrum length. Note that U_0 does not depend on the damping parameter κ_e. Equation (22) is the Madelung energy of a simple cubic lattice of ions of charge Q in a neutralizing background. It is important to keep in mind that Ewald sums are conditionally convergent and that the background is assumed to be spherically symmetric with respect to the position of the inserted ion. The energy U_0 contains the electrostatic self-energy of the background, the interaction energy of ion with the background, and the interaction energy of ion with all of its images.

The change in the electrostatic energy of a charge neutral system with N ions due to the introduction of a replicated test ion at position $\boldsymbol{r}^i$ and a spherical neutralizing background centered on this ion is

$$\Delta U = Q\phi(\boldsymbol{r}^i) + \frac{2\pi Q}{3\varepsilon_w V}\sum_{j=1}^{N}q^j(\boldsymbol{r}^i-\boldsymbol{r}^j)^2 + U_0. \tag{23}$$

The first term in this expression is due to the interaction of ion Q, inserted at positions $\boldsymbol{r}^i$, with the N ions of the original charge neutral system and with their replicas. The electrostatic potential $\phi(\boldsymbol{r}^i)$ is given by Eq. (7). The second term is the interaction energy of the original N ions with the spherical neutralizing background centered on the inserted ion. The resulting quadratic potential results in a linear force produced by the background on each ion. The last term is the interaction energy of the ion Q with its neutralizing background, with its own replicas, as well as the self-energy of the neutralizing background.

The expression can be simplified yielding

$$\Delta U = Q\sum_{\boldsymbol{k}\neq 0}^{\infty}\sum_{j=1}^{N}\frac{4\pi q^j}{\varepsilon_w V|\boldsymbol{k}|^2}\exp\left[-\frac{|\boldsymbol{k}|^2}{4\kappa_e^2}+i\boldsymbol{k}\cdot(\boldsymbol{r}^i-\boldsymbol{r}^j)\right] + Q\sum_{j=1}^{N}q^j\frac{\mathrm{erfc}(\kappa_e|\boldsymbol{r}^i-\boldsymbol{r}^j|)}{\varepsilon_w|\boldsymbol{r}^i-\boldsymbol{r}^j|}+U_0. \quad (24)$$

It is interesting to note that this expression does not depend on **M** for either vacuum or tin-foil boundary condition. This is the case only if the neutralizing background is centered on the inserted ion.

IV. RESULT

We now compare the predictions of the two Widom insertion methods with the μ_t obtained using GCMC simulations. As was discussed in the Sec. I, GCMC does not give us individual chemical potentials of ions, but only the value of μ_t, which we will use as a benchmark to judge the accuracy of the two Widom insertion methods.

We start with symmetric 1:1 electrolyte. In Fig. 2, we present the $\mu_t^{ex} = \mu_+^{ex} + \mu_-^{ex} = 2\mu_+^{ex} = 2\mu_-^{ex}$, obtained using the two Widom insertion methods, compared with the results obtained using the GCMC.

We see that method I results in a very significant deviation from the benchmark GCMC simulation results, while method II is in good agreement. Nevertheless, we see that, even for a fairly large simulation cell of $L = 200$ Å, we have a significant scatter in the data points even after using 50 000 samples to perform averages. On the other hand, we obtain a smooth curve using GCMC already with $L = 200$ Å and only 10 000 samples. In fact, with GCMC, we obtain the same results even with a much smaller simulation cell of $L = 100$ Å. We next repeat the calculations for asymmetric 1:1 electrolyte, with cations of radius 2 Å and anions of radius 3 Å. In Fig. 3(a), we compare the values of μ_t^{ex} obtained using the two Widom methods with the ones obtained using the GCMC. Once again we see that method II is in much better agreement with the GCMC result. Fig. 4(a) shows

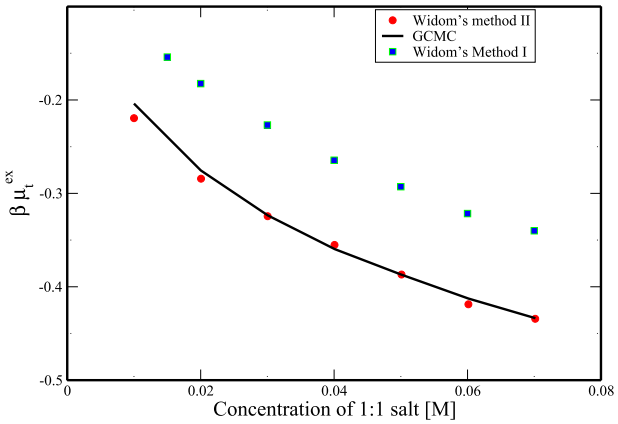

FIG. 2. Comparison of the total excess chemical potential μ_t^{ex} obtained using the two Widom insertion methods and the GCMC simulations. The results of method I are shown with squares and method II with circles. The radii of positive and negative ions are 2 Å.

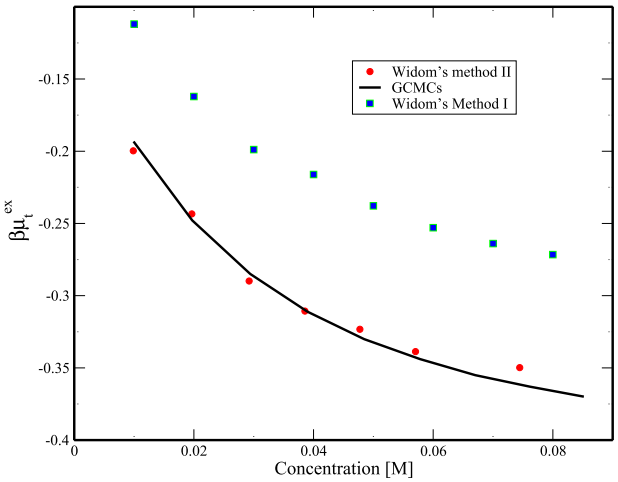

FIG. 3. Comparison of μ_t^{ex} obtained using method II with the GCMC for 1:1 electrolyte with cations of radius 2 Å and anions of 3 Å.

the slow convergence of the Widom insertion method as a function of the number of samples, and Fig. 4(b) shows the convergence of GCMC. In the case of GCMC, we have fixed the fugacity and calculated the average number of particles inside the simulation cell from which we obtain the average concentration. The convergence is much faster for GCMC than for Widom insertion. As we increase the size asymmetry between cations and anion even further, the excess chemical potentials become non-monotonic functions of concentration (see Fig. 5). The reasonably good agreement between method II and GCMC still persists, but the Widom data become noisier for the

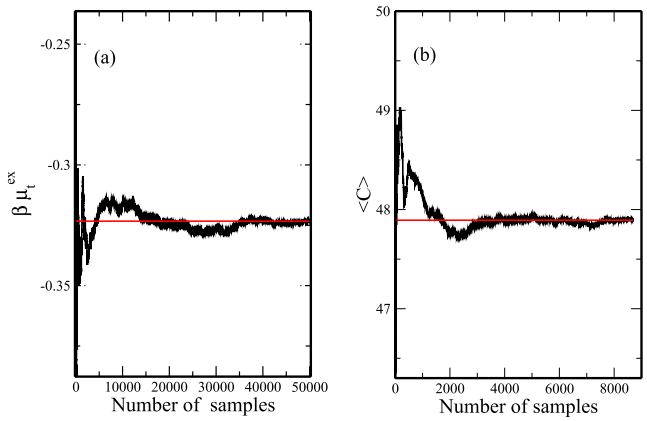

FIG. 4. (a) Convergence of the chemical potential obtained using method II, for 1:1 electrolyte with cations of radius 2 Å and anions of 3 Å at concentration of 48 mM, as a function of the number of samples used. The $\beta\mu_t^{ex}$ converges to −0.32. (b) Convergence of electrolyte concentration in mM, as a function of samples using GCMC simulation with fugacity fixed at 5.9820×10^{-10} Å^{-9}. With this value, we obtain $\beta\mu_t^{ex} = -0.32$ and the concentration 47.4 mM. We see that convergence is much faster for GCMC than for Widom insertion, both in terms of the CPU time, since one can use a smaller simulation cell, and also in terms of the number of samples needed to calculate the averages.

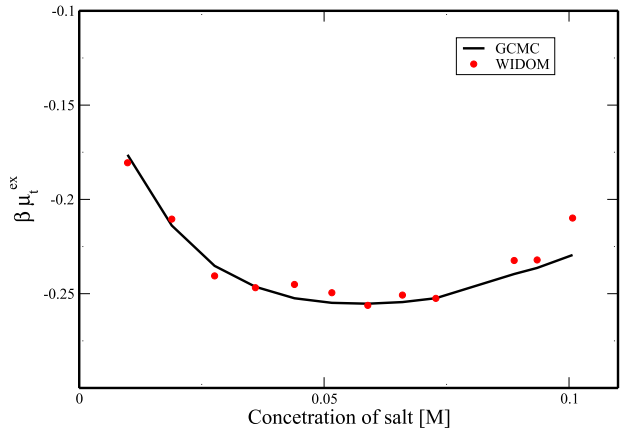

FIG. 5. Comparison of μ_t^{ex} obtained using method II with the GCMC simulation results for 1:1 electrolyte with cation of radius 2 Å and anions of 4 Å. For large size asymmetry between cations and anions, the chemical potential is no longer a monotonic function of electrolyte concentration.

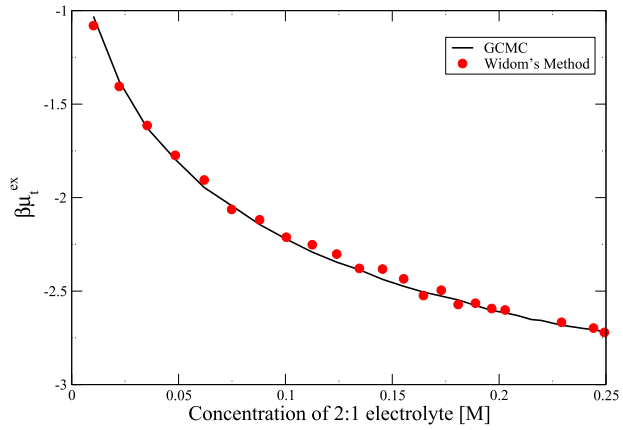

FIG. 6. Comparison of the excess chemical potential μ_t^{ex} obtained using GCMC simulations with Widom method II for size symmetric 2:1 electrolyte with ions of radius 2 Å.

same number of samples. Finally, in Fig. 6, we compare method II with GCMC for size symmetric 2:1 electrolyte, with ions of radius 2 Å. In this case, $\mu_t^{ex} = \mu_+^{ex} + 2\mu_-^{ex}$. Again, we see a good agreement between GCMC and method II.

TABLE I. Individual and total chemical potentials obtained using method II compared with GCMCs results for 2:1 electrolyte.

c (mM)	$\beta\mu_{++}$	$\beta\mu_{-}$	$\beta\mu_{++} + 2\beta\mu_{-}$	$\beta\mu_{t}$
10	−0.700	−0.189	−1.080	−1.030
60	−1.220	−0.342	−1.905	−1.945
100	−1.439	−0.386	−2.211	−2.222
145	−1.567	−0.407	−2.381	−2.437
172	−1.651	−0.421	−2.495	−2.526
202	−1.739	−0.430	−2.600	−2.615
252	−1.834	−0.433	−2.701	−2.722

To more clearly see the degree of agreement between the Widom insertion method and GCMC, in Table I, we present the individual chemical potentials of cations and anions of 2:1 electrolyte calculated using method II. We also compare the resulting values of μ_t with the ones obtained using GCMC. We see that even with 50 000 samples, the agreement is only to two significant figures.

V. CONCLUSION

We have explored the use of the Widom insertion method for calculating the chemical potential of individual ions in computer simulations with Ewald summation. Two approaches were considered. In the first approach, an individual ion is inserted into a periodically replicated overall charge neutral system representing an electrolyte solution. In the second approach, an inserted ion is also periodically replicated, resulting in a macroscopic violation of the overall charge neutrality. To overcome this problem, a neutralizing background must be introduced simultaneously with the ion. This results in a linear force that the background exerts on all the ions. Comparing the results of the two methods, we find that the second approach is in much better agreement with the benchmark GCMC simulations for the total chemical potential of the ions μ_t. This is consistent with the results obtained using the minimum image simulations, which were also found to require a neutralizing background to improve convergence[30,60] as well as with the simulations of ionic solvation.[61] We find that to be accurate: the Widom insertion method requires very large simulation cells. Apparently, for only very large cells, the contribution of the background to the chemical potential becomes negligible. To produce reasonably accurate values of the chemical potential of individual ions, a very large number of samples must also be used. Therefore, in applications that do not require knowledge of the individual ionic chemical potentials, but only of μ_t, the GCMC approach is by far more practical.

The significant difference between Widom's methods I and II is quite surprising. Its origin can be traced back to the careful limit of the $k = 0$ term of Ewald potential [see Eqs. (7) and (8)]. The limit results in a term quadratic in ion positions as well as **M** dependent contribution, Eq. (8). These terms are usually neglected appealing to tin-foil boundary condition. However, tin-foil will only remove the M dependent term, while the quadratic term still remains. Indeed, the quadratic term is of fundamental importance when studying non-neutral systems, such as ions confined between like charged plates (see, for example, Ref. 45). It is precisely the quadratic term that leads to the deviation between Widom's methods I and II. When using Widom method II, the quadratic term cancels precisely by the interaction with a neutralizing background that is introduced together with the inserted ion [see Eq. (23)].

ACKNOWLEDGMENTS

This work was partially supported by the CNPq, CAPES, and National Institute of Science and Technology Complex Fluids INCT-FCx. The authors acknowledge the Instituto de Física e Matemática, UFPel, for the use of computer resources.

AUTHOR DECLARATIONS

Conflict of Interest

The authors have no conflicts to disclose.

DATA AVAILABILITY

The data that support the findings of this study are available from the corresponding author upon reasonable request.

REFERENCES

[1] W. M. Latimer, K. S. Pitzer, and C. M. Slansky, "The free energy of hydration of gaseous ions, and the absolute potential of the normal calomel electrode," J. Chem. Phys. **7**, 108–111 (1939).

[2] E. Waisman and J. L. Lebowitz, "Mean spherical model integral equation for charged hard spheres I. Method of solution," J. Chem. Phys. **56**, 3086–3093 (1972).

[3] R. Triolo, J. R. Grigera, and L. Blum, "Simple electrolytes in the mean spherical approximation," J. Phys. Chem. **80**, 1858–1861 (1976).

[4] M. Fushiki, "A hypernetted chain structure factor for charged colloidal dispersions," J. Chem. Phys. **89**, 7445–7453 (1988).

[5] P. J. in't Veld, A. E. Ismail, and G. S. Grest, "Application of Ewald summations to long-range dispersion forces," J. Chem. Phys. **127**, 144711 (2007).

[6] A. Delville and R. J.-M. Pellenq, "Electrostatic attraction and/or repulsion between charged colloids: A (NVT) Monte-Carlo study," Mol. Simul. **24**, 1–24 (2000).

[7] M. Deserno and C. Holm, "How to mesh up Ewald sums. I. A theoretical and numerical comparison of various particle mesh routines," J. Chem. Phys. **109**, 7678–7693 (1998).

[8] Z. Wang and C. Holm, "Estimate of the cutoff errors in the Ewald summation for dipolar systems," J. Chem. Phys. **115**, 6351–6359 (2001).

[9] J. de Joannis, A. Arnold, and C. Holm, "Electrostatics in periodic slab geometries. II," J. Chem. Phys. **117**, 2503–2512 (2002).

[10] A. Bakhshandeh, A. P. Dos Santos, A. Diehl, and Y. Levin, "Isothermal adsorption of polyampholytes on charged nanopatterned surfaces," J. Chem. Phys. **151**, 084101 (2019).

[11] A. Bakhshandeh and M. Segala, "Adsorption of polyelectrolytes on charged microscopically patterned surfaces," J. Mol. Liq. **294**, 111673 (2019).

[12] A. Bakhshandeh, A. P. Dos Santos, and Y. Levin, "Efficient simulation method for nano-patterned charged surfaces in an electrolyte solution," Soft Matter **14**, 4081–4086 (2018).

[13] P. Linse, "Simulation of charged colloids in solution," in *Advanced Computer Simulation Approaches for Soft Matter Sciences* (Springer, 2005), Vol. 2, pp. 111–162.

[14] A. Cuetos, A. P. Hynninen, J. Zwanikken, R. van Roij, and M. Dijkstra, "Layering in sedimentation of suspensions of charged colloids: Simulation and theory," Phys. Rev. E **73**, 061402 (2006).

[15] J. Kolafa and J. W. Perram, "Cutoff errors in the Ewald summation formulae for point charge systems," Mol. Simul. **9**, 351–368 (1992).

[16] Y. Levin, "Electrostatic correlations: From plasma to biology," Rep. Prog. Phys. **65**, 1577 (2002).

[17] S. A. Barr and A. Z. Panagiotopoulos, "Grand-canonical Monte Carlo method for Donnan equilibria," Phys. Rev. E **86**, 016703 (2012).

[18] B. Widom, "Some topics in the theory of fluids," J. Chem. Phys. **39**, 2808–2812 (1963).

[19] D. J. Adams, "Chemical potential of hard-sphere fluids by Monte Carlo methods," Mol. Phys. **28**, 1241–1252 (1974).

[20] K. S. Shing and K. E. Gubbins, "The chemical potential in dense fluids and fluid mixtures via computer simulation," Mol. Phys. **46**, 1109–1128 (1982).

[21] D. Frenkel, G. C. A. M. Mooij, and B. Smit, "Novel scheme to study structural and thermal properties of continuously deformable molecules," J. Phys.: Condens. Matter **4**, 3053 (1992).

[22] R. D. Groot, "Mesoscopic simulation of polymer-surfactant aggregation," Langmuir **16**, 7493–7502 (2000).

[23] R. P. A. Dullens, D. G. A. L. Aarts, W. K. Kegel, and H. N. W. Lekkerkerker, "The Widom insertion method and ordering in small hard-sphere systems," Mol. Phys. **103**, 3195–3200 (2005).

[24] B. M. Mladek and D. Frenkel, "Pair interactions between complex mesoscopic particles from Widom's particle-insertion method," Soft Matter **7**, 1450–1455 (2011).

[25] I. Nezbeda and J. Kolafa, "A new version of the insertion particle method for determining the chemical potential by Monte Carlo simulation," Mol. Simul. **5**, 391–403 (1991).

[26] D. Boda, J. Giri, D. Henderson, B. Eisenberg, and D. Gillespie, "Analyzing the components of the free-energy landscape in a calcium selective ion channel by Widom's particle insertion method," J. Chem. Phys. **134**, 055102 (2011).

[27] B. Widom, "Structure of interfaces from uniformity of the chemical potential," J. Stat. Phys. **19**, 563–574 (1978).

[28] B. R. Svensson and C. E. Woodward, "Widom's method for uniform and non-uniform electrolyte solutions," Mol. Phys. **64**, 247–259 (1988).

[29] J. C. d. S. L. Maciel, C. R. A. Abreu, and F. W. Tavares, "Chemical potentials of hard-core molecules by a stepwise insertion method," Braz. J. Chem. Eng. **35**, 277–288 (2018).

[30] P. Sloth and T. S. Sørensen, "Monte Carlo calculations of chemical potentials in ionic fluids by application of Widom's formula: Correction for finite-system effects," Chem. Phys. Lett. **173**, 51–56 (1990).

[31] B. Xu, X. Liu, and B. Zhou, "Calculation methods of solution chemical potential and application in emulsion microencapsulation," Molecules **26**, 2991 (2021).

[32] D. Frenkel, B. Smit, and M. A. Ratner, *Understanding Molecular Simulation: From Algorithms to Applications* (Academic Press, San Diego, 1996), Vol. 2.

[33] S. Albo and E. A. Müller, "On the calculation of supercritical fluid-solid equilibria by molecular simulation," J. Phys. Chem. B **107**, 1672–1678 (2003).

[34] S. J. Pai and Y. C. Bae, "Solubility of solids in supercritical fluid using the hard-body expanded virial equation of state," Fluid Phase Equilib. **362**, 11–18 (2014).

[35] P. Gestoso and M. Meunier, "Barrier properties of small gas molecules in amorphous *cis*-1, 4-polybutadiene estimated by simulation," Mol. Simul. **34**, 1135–1141 (2008).

[36] J. Carrero-Mantilla, "Simulation of the (vapor + liquid) equilibria of binary mixtures of benzene, cyclohexane, and hydrogen," J. Chem. Thermodyn. **40**, 271–283 (2008).

[37] P. H. Hünenberger and J. A. McCammon, "Ewald artifacts in computer simulations of ionic solvation and ion–ion interaction: A continuum electrostatics study," J. Chem. Phys. **110**, 1856–1872 (1999).

[38] R. M. Levy and E. Gallicchio, "Computer simulations with explicit solvent: Recent progress in the thermodynamic decomposition of free energies and in modeling electrostatic effects," Annu. Rev. Phys. Chem. **49**, 531–567 (1998).

[39] S. H. Saravi and A. Z. Panagiotopoulos, "Individual ion activity coefficients in aqueous electrolytes from explicit-water molecular dynamics simulations," J. Phys. Chem. B **125**, 8511–8521 (2021).

[40] P. P. Ewald, "Ewald summation," Annu. Phys. **369**, 1–2 (1921).

[41] T. Darden, D. York, and L. Pedersen, "Particle mesh Ewald: An N log(N) method for Ewald sums in large systems," J. Chem. Phys. **98**, 10089–10092 (1993).

[42] A. Bakhshandeh, A. P. dos Santos, A. Diehl, and Y. Levin, "Interaction between random heterogeneously charged surfaces in an electrolyte solution," J. Chem. Phys. **142**, 194707 (2015).

[43] J. P. Valleau and L. K. Cohen, "Primitive model electrolytes. I. Grand canonical Monte Carlo computations," J. Chem. Phys. **72**, 5935–5941 (1980).

[44] M. P. Allen and D. J. Tildesley, *Computer Simulation of Liquids* (Oxford University Press, 2017).

[45] A. P. dos Santos, M. Girotto, and Y. Levin, "Simulations of Coulomb systems with slab geometry using an efficient 3D Ewald summation method," J. Chem. Phys. **144**, 144103 (2016).

[46] V. Ballenegger, A. Arnold, and J. J. Cerdá, "Simulations of non-neutral slab systems with long-range electrostatic interactions in two-dimensional periodic boundary conditions," J. Chem. Phys. **131**, 094107 (2009).

[47] V. Ballenegger, "Communication: On the origin of the surface term in the Ewald formula," J. Chem. Phys. **140**, 161102 (2014).

[48] E. R. Smith, "Electrostatic energy in ionic crystals," Proc. R. Soc. London, Ser. A **375**, 475–505 (1981).

[49]I.-C. Yeh and M. L. Berkowitz, "Ewald summation for systems with slab geometry," J. Chem. Phys. **111**, 3155–3162 (1999).
[50]S. Yi, C. Pan, and Z. Hu, "Note: A pairwise form of the Ewald sum for non-neutral systems," J. Chem. Phys. **147**, 126101 (2017).
[51]I. M. Telles, R. K. Bombardelli, A. P. dos Santos, and Y. Levin, "Simulations of electroosmotic flow in charged nanopores using dissipative particle dynamics with Ewald summation," J. Mol. Liq. **336**, 116263 (2021).
[52]S. W. De Leeuw and J. W. Perram, "Computer simulation of ionic systems. Influence of boundary conditions," Physica A **107**, 179–189 (1981).
[53]J. S. Ho/ye and E. Lomba, "Mean spherical approximation (MSA) for a simple model of electrolytes. I. Theoretical foundations and thermodynamics," J. Chem. Phys. **88**, 5790–5797 (1988).
[54]C.-H. Ho, H.-K. Tsao, and Y.-J. Sheng, "Interfacial tension of a salty droplet: Monte Carlo study," J. Chem. Phys. **119**, 2369–2375 (2003).
[55]Y. Levin and M. E. Fisher, "Criticality in the hard-sphere ionic fluid," Physica A **225**, 164–220 (1996).
[56]E. Waisman and J. L. Lebowitz, "Mean spherical model integral equation for charged hard spheres. II. Results," J. Chem. Phys. **56**, 3093–3099 (1972).
[57]L. Blum, "Mean spherical model for asymmetric electrolytes. I. Method of solution," Mol. Phys. **30**, 1529–1535 (1975).
[58]N. F. Carnahan and K. E. Starling, "Equation of state for nonattracting rigid spheres," J. Chem. Phys. **51**, 635–636 (1969).
[59]N. F. Carnahan and K. E. Starling, "Thermodynamic properties of a rigid-sphere fluid," J. Chem. Phys. **53**, 600–603 (1970).
[60]A. Malasics and D. Boda, "An efficient iterative grand canonical Monte Carlo algorithm to determine individual ionic chemical potentials in electrolytes," J. Chem. Phys. **132**, 244103 (2010).
[61]G. Hummer, L. R. Pratt, and A. E. García, "Free energy of ionic hydration," J. Phys. Chem. **100**, 1206–1215 (1996).